Article:
Chu, F, Li, S, Ni, Z et al. (1 more author) (2020) Departure Velocity of Rolling Droplet Jumping. Langmuir, 36 (14). pp. 3713-3719. ISSN 0743-7463

https://doi.org/10.1021/acs.langmuir.0c00185

Departure velocity of rolling droplet jumping

Fuqiang Chu[1,‡,]*, *Shaokang Li*[1,‡], *Zhongyuan Ni*[1], *Dongsheng Wen*[1,2,]*

[1]School of Aeronautic Science and Engineering, Beihang University, Beijing 100191, China

[2]School of Chemical and Process Engineering, University of Leeds, Leeds LS2 9JT, UK

Abstract: Droplet jumping phenomenon widely exists in the fields of self-cleaning, anti-frosting and heat transfer enhancement. Numerous studies have been reported on the static droplet jumping while the rolling droplet jumping still remains unnoticed although it is very common in practice. Here, we used the volume of fluid (VOF) method to simulate the droplet jumping induced by coalescence of a rolling droplet and a stationary one with corresponding experiments conducted to validate the correctness of the simulation model. The departure velocity of the jumping droplet was mainly concerned here. The results show that when the center velocity of the rolling droplet ($V_0 = \omega R$, where ω is the angular velocity of the rolling droplet and R is the droplet radius) is fixed, the vertical departure velocity satisfies a power law which can be expressed as $V_{z,\,depar} = aR^b$. When the droplet radius is fixed, the vertical departure velocity first decreases, and then increases if the center velocity exceeds a critical value. Interestingly, the critical center velocity is demonstrated to be approximately 0.76 times of the capillary-inertial velocity, corresponding to a constant Weber number of 0.58. Different from the vertical departure velocity, the horizontal departure velocity is basically proportional to the center velocity of the rolling droplet. These results deepen the understanding of the droplet jumping physics, which shall further promote related applications in engineering fields.

Keywords: Droplet jumping; VOF; Rolling droplet; Departure velocity;

Introduction

Droplet jumping phenomenon on superhydrophobic surfaces has received much attention in recent years. In 2009, Boreyko and Chen first reported this phenomenon which was triggered by coalescence of two condensed water droplets, and quantitatively predicted the jumping velocity via capillary-inertial scale analysis.[1] Following that, extensive studies have been performed to investigate the droplet jumping mechanism.[2-12] Due to its capacity for droplet self-removing, the droplet jumping phenomenon could be widely applied in many engineering fields, such as self-cleaning, anti-frosting, defrosting, heat transfer enhancement and hotspot cooling.[13-23] The jumping velocity, *i.e.*, the departure velocity, is an important indicator for the droplet jumping phenomenon, which reflects

its practical application value. Thus, predicting and controlling the droplet departure velocity have become the pursuit of many researches.

The droplet jumping can be divided into two types based on different triggering conditions, *i.e.*, triggered by coalescence of stationary droplets and by coalescence of moving droplets. Regarding the first type, for the equal-sized static droplet jumping, when the droplet radius is larger than the cut-off radius, the departure velocity can be scaled by the capillary-inertial velocity, $u_{ci}=(\sigma/\rho R)^{0.5}$, with a proportionality factor between 0.2 to 0.3.[4, 24, 25] Droplet size mismatch also affects the droplet jumping dynamics with numerous works reported to elucidate the relationship between the departure velocity and droplet radius ratio.[7, 26, 27] In addition to the droplet conditions, the roughness length scale of the superhydrophobic surface changes the departure velocity greatly, and there is an optimal length to maximize the departure velocity.[28-31] Compared with the first type of the droplet jumping, research on the second type jumping is much less. For the second type, two cases are concerned currently. One is the multi-hop jumping, and its departure velocity mainly depends on the impacting position and velocity of the back-flow droplet.[5, 10, 32, 33] Another is the jumping triggered by two droplets moving towards each other with the same approaching velocity. In this case, the departure velocity could be affected only when the approaching velocity is large enough.[25, 34]

It should be noted that it is also common to see a moving droplet horizontally impacting on a stationary droplet, resulting in a unique jumping behavior (See the supplemental video by Boreyko and Chen for an example[1]). However, no one has noticed this case yet, though this case seems to be more promising, especially for those applications need precise droplet regulation such as hot-spot cooling. Clarifying the effects of the moving droplet velocity can not only deepen the understanding of the droplet jumping dynamics, but also provide significant guidance for the droplet regulation, which further broadens the application of the droplet jumping in wider fields like microfluidics.[35, 36] As for the moving droplet, there are two moving forms including sliding and rolling. In our another recent work, we have discussed the effect of the moving velocity of sliding droplets.[37] However, compared with the sliding, the rolling form is more common as the droplet prefers to roll on the superhydrophobic surface once the incline angle of the surface exceeds its rolling angle.[38, 39] Thus, in this work, we paid our attention on the droplet jumping induced by coalescence of a rolling droplet and a stationary one, which may be the first work on the topic of rolling droplet jumping.

Numerical model

Numerical method was mainly adopted to investigate the rolling droplet jumping phenomenon. The interFoam solver in OpenFOAM was used to perform the simulation. This solver is based on the volume of fluid method (VOF) and tracks the liquid-gas interface by setting the volume fraction in each grid. In the droplet jumping simulation, it

is necessary to consider the effect of the dynamic contact angle. The Kistler's dynamic contact angle model was chosen and compiled in the interFoam solver as a boundary condition. Please refer to our recent work for the detailed equations in the numerical model.[37]

Figure 1(a) shows the schematic of rolling droplet jumping. The left droplet has a clockwise angular velocity and moves towards the stationary droplet, and then the merged droplet jumps up because of coalescence. Figure 1(b) shows the computational domain with a size of 3×3×3 mm. The grid number was set to 150×150×150 according to our recent work about sliding droplet jumping.[37] The contact angle of the bottom solid wall was set to 180° and other boundaries were pressure-outlet conditions. To save computing resources, we set the time to the initial time when two droplets started to contact each other. In the simulation, the main influence factors include the droplet radius (from 40 to 300 μm) and the angular velocity of the rolling droplet. To simplify the analysis, we used the center velocity of the rolling droplet to describe its angular velocity which can be expressed as $V_0=\omega R$, where ω is the angular velocity and R is the droplet radius. The center velocity of the rolling droplet varies from 0 to 2 m/s.

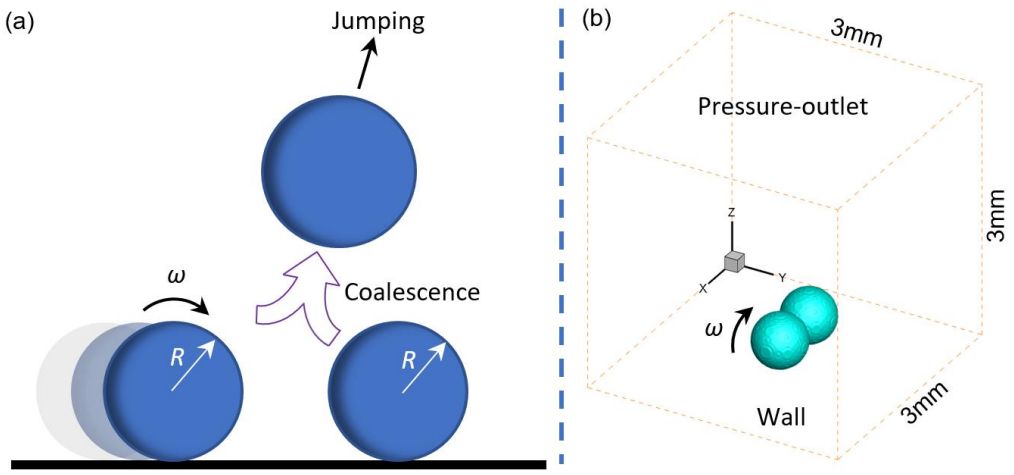

Fig. 1. (a) Schematic diagram of rolling droplet jumping. The left droplet has a clockwise angular velocity, moving towards the stationary droplet, and the merged droplet jumps up after coalescence. The angular velocity of the left droplet is ω, and the two droplets have equal radius, labelled as R. (b) Computational domain and boundary conditions. The computational domain is a cubic with side lengths of 3 mm. The contact angle of the bottom solid wall is 180°, *i.e.*, ideally superhydrophobic. The other boundaries are all pressure-outlet conditions. The distance between the droplet and the boundary is large enough to prevent the boundary from affecting the jumping dynamics.

Rolling droplet jumping experiment

To validate the correctness of the numerical model, we performed rolling droplet jumping experiments. The

experimental surface is a kind of Al-based superhydrophobic surface fabricated by chemical etching-deposition method reported in our previous works.[40-42] The experimental surface has flower-like hierarchical structures, which is the key point for its superhydrophobicity. The measurement shows that the static contact angle of the experimental surface is 159.7±1.0° with a rolling contact angle less than 3°, indicating that droplet can easily roll on the superhydrophobic surface. The detailed scanning electron microscope image and contact angle measurement result are exhibited in Fig. 2.

Figure 2 also shows the schematic of the experiment system for the rolling droplet jumping. The injection system, consisting of a syringe pump, an injector and a thin needle (0.31 mm diameter), was used to produce two stationary droplets on the surface. Then, an empty injector with a thin needle (0.31 mm diameter) generated a tiny airflow to blow the upper part of one droplet and the airflow shearing effect causes the droplet to roll towards another. A high-speed camera recorded the entire droplet merging and jumping process. We confirm that the blowed droplet is rolling after comparing the droplet morphologies during jumping in this work with those during the sliding droplet jumping,[37] as mentioned below.

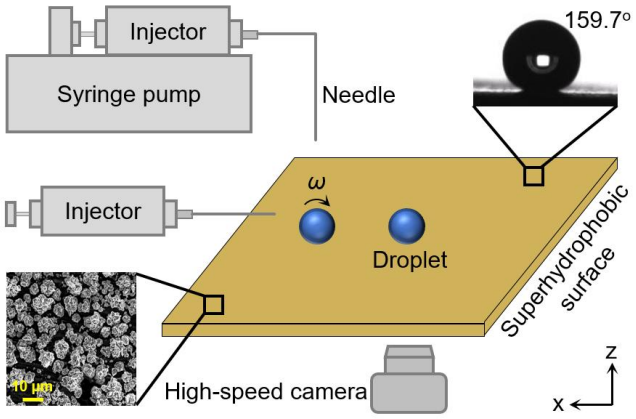

Fig. 2. Experimental surface and experimental system. The experimental surface is a kind of Al-based superhydrophobic surface with flower-like hierarchical structures and a static contact angle of 159.7°. The experimental system consists of an injection system to produce small droplets, an empty injector with a thin needle to generate tiny airflow to make stationary droplet roll, and a high-speed camera to record images.

Results and discussion

Droplet morphological changes

Figure 3(a) shows the simulated droplet morphological changes during the rolling jumping process. At $t^*=0$ (t^* is the dimensionless time scaled by coalescence time τ, $\tau=(\rho R^3/\sigma)^{0.5}$), the left droplet with a clockwise angular velocity impacts on the stationary droplet. Then two droplets begin to merge with each other through the expansion

of the liquid bridge. Due to the effect of initial angular velocity, the left side of the merged droplet has an obvious lift at t^*=1.08, rather than remaining level which occurs during sliding droplet jumping (see the graphical abstract in our another work for comparison[37]). Moreover, the merged droplet always keeps a clockwise rolling motion trend, even when it jumps up from the surface; while for the sliding droplet jumping,[37] the merged droplet does not have any rotational motion, although it also departs from the surface obliquely. Figure 3(b) shows the experimental droplet morphological changes during rolling droplet jumping, which agree well with the simulation results.

In addition, there are also obvious differences between the droplet jumping by two droplets with initial opposite velocities and the rolling droplet jumping, regarding the droplet morphological changes. For the former case, according to the results by Liu *et al*.[25] or Chen and Lian,[34] the droplet morphology maintains symmetrical all through the coalescence and jumping process, and the droplet jumps up perpendicularly; while for the rolling droplet jumping concerned here, the droplet morphology is asymmetric and the jumping direction become oblique.

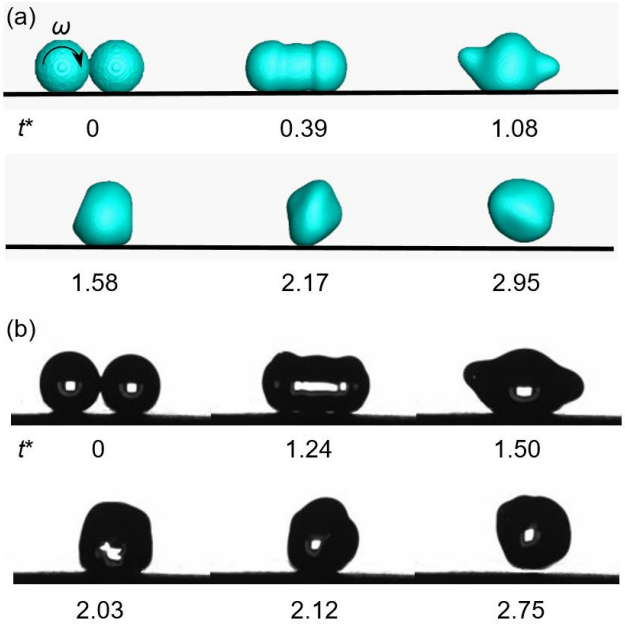

Fig. 3. Comparison of droplet morphological changes between (a) simulation and (b) experimental results. In the simulation and the experiments, the weber numbers ($We=\rho V_0^2 R/\sigma$) are set the same for comparability. In the simulation, the rolling droplet has a radius of 300 μm and a center velocity of 0.335 m/s with We=0.46. In the experiment, the rolling droplet radius is 1.5 mm and its center velocity is 0.15 m/s.

However, in Fig. 3, one may notice that the droplet morphology evolution at the initial stage in the simulation is faster than in the experiment. This is because the current model (VOF model) cannot simulate the droplet squeeze phenomenon in the experiments that two droplets do not merge immediately when they contact, but squeeze each other first. In the experiments, as shown in Fig. 4, the squeezing process persists until t^*=1.05. The droplet squeeze

phenomenon is a kind of interface behavior that probably relates to energy of real interface, it may also due to the interaction between air and droplet (such as the air entrapment at the droplet contact point).[43, 44] Actually, this droplet squeeze phenomenon is very interesting but less mentioned previously. We infer that targeted research on the droplet squeezing mechanism could change our previous perception on the droplet coalescence dynamics and help to reveal new coalescence mechanisms, and we will start a research in our next work. Though the squeeze phenomenon delays the coalescence of the two droplets, the resulted extrusion deformation increases the potential energy of coalescence, which will result in a faster merging process once the coalescence begins. The compromise between the delayed coalescence and the accelerated merging makes the final droplet departure times obtained from simulation and experiment consistent (Fig. 3). In other words, the simulated departure characteristics of the rolling droplet jumping are still reliable though the simulation model cannot simulate the droplet squeeze phenomenon.

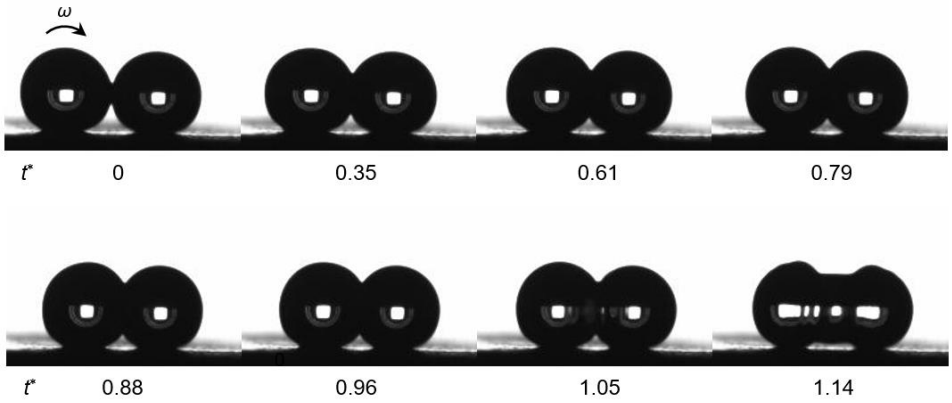

Fig. 4. Time-lapse images of the droplet squeeze phenomenon before coalescence of the rolling droplet and the static one. The two droplets do not merge immediately when they contact but squeeze each other first. The squeezing process persists until t^*=1.05. The dimensionless time corresponds to the time of Fig. 3(b).

Figure 5 shows the velocity vectors inside the droplets at times corresponding to those in Fig. 3(a). There are clockwise angular velocity vectors in the left droplet at the initial moment (t^*=0), which, on the one hand, accelerate the expansion of the left-part liquid bridge (t^*=0.39), on the other hand, cause the left side of the droplet to lift up (t^*=1.08). In contrast, the right droplet evolves normally under capillary pressure. The combination of the different motion trends between the left and the right parts of the merging droplet yields unique departure characteristics that the merged droplet jumps up from the surface obliquely with angular velocity remaining inside the droplet (t^*=2.95).

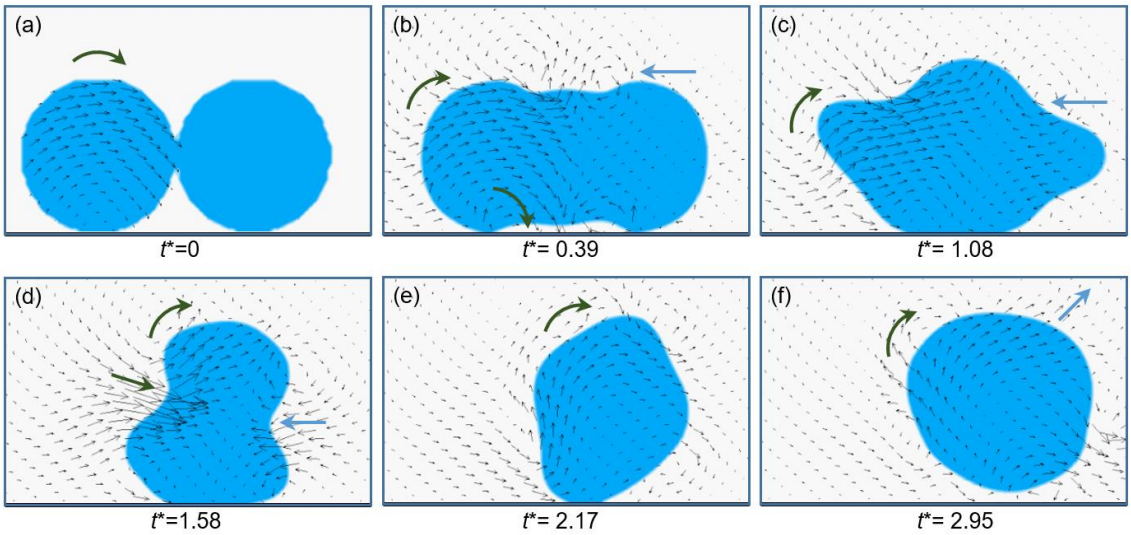

Fig. 5. Velocity vectors inside the droplets at times corresponding to those in Fig. 3(a). The left droplet has clockwise rotation velocity vectors, and these rotation velocity vectors persist throughout the entire jumping process. Coupling of the effect of rotation velocity and the coalescence effect results in unique motion trends and departure characteristics of the merged droplet. Green arrows represent the effect of rotation velocity and blue arrows represent the normal coalescence effect.

Vertical departure velocity

To analyze the departure characteristics of the merged droplets quantitatively, relationship between vertical departure velocity (*i.e.*, vertical velocity component of the merged droplet as it just departs from the surface) and droplet radius under various center velocities is drawn in Fig. 6(a). The black solid curve represents the theoretical departure velocity by capillary-inertial law for the static-droplet-coalescence induced jumping, known as $0.2u_{ci}$. For water droplets, the theoretical curve is about $1.706R^{-0.5}$ (the unit of radius is micron). When angular velocity is added to the left droplet, the departure velocity still satisfies this form, denoted as aR^b, where a and b are constants. As the center velocity of the rolling droplet increases, the constant b increases (In Fig. 6(a), the constant b increases monotonously from -0.5 to -0.1 when the center velocity of the rolling droplet varies from 0 m/s to 2 m/s). In addition, the chart in the lower left corner in Fig. 6(a) shows the relative deviation between the simulated vertical departure velocities and the theoretical value by capillary-inertia law. When the center velocity is larger than 0.3 m/s (the dotted line in the chart), the deviation begins to increase significantly, indicating that the capillary-inertia law cannot predict the vertical departure velocity any more.

To explain the effect of the center velocity more clearly, the relationship between vertical departure velocity and center velocity at different droplet radii is shown in Fig. 6(b). As seen, when the center velocity increases, the vertical departure velocity first decreases and then increases. Based on this trend, two regions are divided, including

descending region and ascending region. The center velocity on the junction of the two regions is regarded as the critical center velocity, V_c. The critical center velocity decreases continuously as the droplet radius increases.

For the droplet jumping induced by coalescence of static droplets, the duration time from coalescence to departure can be expressed as $t \approx 2.2\tau$ according to the recent work by Yan *et al.*,[45] where τ is the coalescence time expressed as $(\rho R^3/\sigma)^{0.5}$. According to the theorem of momentum, the average merging velocity of the static droplet under capillary pressure ($\Delta p=2\sigma/R$) is given by

$$U = \frac{\Delta P \cdot S \cdot t}{m} \tag{1}$$

where S is the action area of the capillary pressure and m is the droplet mass. Substituting the expressions of Δp, S, t, and m into Eq. (1) gives

$$U \approx 3.3\sqrt{\frac{\sigma}{\rho R}} \tag{2}$$

In other words, U is approximately equal to $3.3u_{ci}$. Then we calculated the ratio of the simulated critical center velocity, V_c, to the average merging velocity of the static droplet, U, at different droplet radii, and showed the results in Fig. 6(c) that the ratio fluctuates around 0.23 with a deviation of 0.01. Therefore, the critical center velocity of the rolling droplet can be estimated as

$$V_c \approx 0.76u_{ci} \tag{3}$$

Equation (3) is drawn in Fig. 6(b) as the black curve, and the result shows that it can well represent the boundary between the descending region and ascending region. Further, substituting Eq. (3) into the formula of Weber number ($We=\rho V_c^2 R/\sigma$) gives that We = 0.5776. In other words, the critical center velocity of rolling droplet corresponds to a constant $We \approx 0.58$. As known, the Weber number measures the relative importance of the fluid's inertia compared to its surface tension. For the rolling droplet jumping, when the Weber number is larger than 0.58, the inertial of the rolling droplet plays a more and more important role, indicating that the increased kinetic energy of the rolling droplet could increase the vertical departure velocity; otherwise, when the Weber number is smaller than 0.58, the released surface energy by coalescence still dominates the rolling droplet jumping, and the increasing center velocity of rolling droplet actually increases viscous dissipation, resulting in a decrease of the vertical departure velocity.

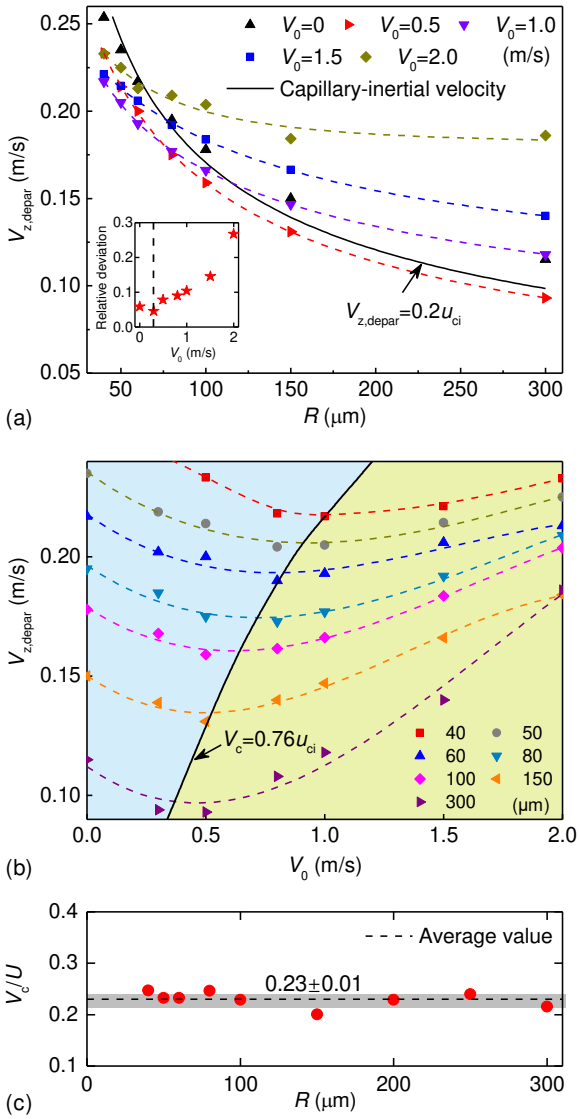

Fig. 6. (a) Relationship between vertical departure velocity and droplet radius under various center velocities. At a certain center velocity, the vertical departure velocity gradually decreases with increasing droplet radius. The vertical departure velocity deviations between the simulated value and the theoretical value by capillary-inertia law are also shown in the lower left corner. (b) Relationship between center velocity of the rolling droplet and vertical departure velocity under different droplet radii. The vertical departure velocity decreases in the blue region and increases in the yellow region. The black curve represents the theoretical critical center velocity (V_0=0.76u_{ci}) which can precisely distinguish the descending region and the ascending region. (c) The ratio of the simulated critical center velocity, V_c, to the average merging velocity of the static droplet, U, under different droplet radii. The ratio is approximately constant at 0.23 with a deviation of 0.01.

Horizontal departure velocity and departure angle

The rolling velocity of the moving droplet makes the merged droplet jump up obliquely, *i.e.*, the merged droplet

has both vertical and horizontal velocity components when it departs from the surface. The horizontal departure velocity is also concerned and its relationship with the center velocity of the rolling droplet at different droplet radii is shown in Fig. 7(a). Similar to the sliding droplet jumping discussed in our another work,[37] the horizontal departure velocity ($V_{x,depar}$) and the center velocity is directly proportional. The proportionality coefficients change from 0.37 to 0.47 when the droplet radius increases from 40 μm to 300 μm. But the proportionality coefficient does not vary linearly with the droplet radius, as the small chart in the upper left corner in Fig. 7(a) shown.

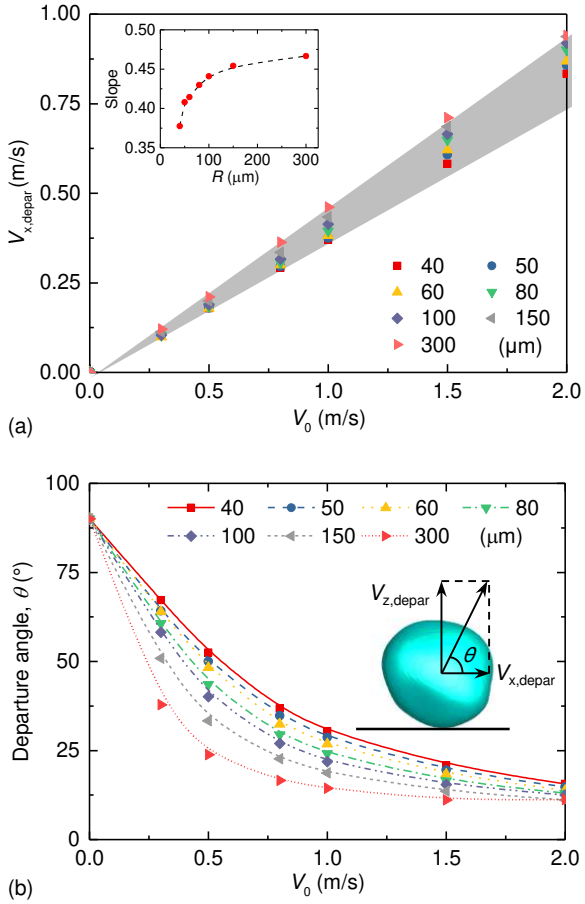

Fig. 7. (a) Relationship between the horizontal departure velocity and the center velocity at different droplet radii. The simulated radius range is from 40 μm to 300 μm. The horizontal departure velocity ($V_{x,depar}$) and the center velocity is directly proportional, and the proportionality coefficient increases with increasing droplet radius but the tendency is not linear. (b) Relationship between the departure angle and the center velocity at different droplet radii. The departure angle of the merged droplet decreases with increasing droplet center velocity and droplet radius.

With determined vertical and horizontal departure velocities, the jumping direction of the merged droplet can be calculated. Here, the departure angle, θ, is used to indicate the jumping direction. The departure angle means the angle between the jumping direction and the horizontal direction, and Fig. 7(b) shows the relationship between the

departure angle and the center velocity at different droplet radii. As shown, the departure angles decrease with increasing center velocities of the rolling droplets, indicating that the jumping directions become more and more parallel to the surface. In addition, at a certain droplet center velocity, larger droplet results in smaller departure angle. All these results demonstrate the controllability of the rolling droplet jumping and provide significant guidance for related engineering applications.

Conclusions

In conclusion, we adopted the VOF method to simulate the phenomenon of rolling droplet jumping (*i.e.*, the jumping induced by coalescence of a rolling droplet and a static one) with the simulation model validated against our own experiments. We extracted the departure velocity when the droplet just jumps up from the simulation, and concluded that the angular velocity of the rolling droplet has a great effect on the subsequent coalescence dynamics, which then influences the droplet departure. For convenience, the center velocity of the rolling droplet was used to describe the droplet rolling. When the center velocity of the rolling droplet is constant, the vertical departure velocity shows a power function of the droplet radius. When the droplet radius is constant, as the center velocity increases, the vertical departure velocity first decreases and then increases. Moreover, the critical center velocity, V_c, which corresponds to the minimum vertical departure velocity, satisfies a constant relation with the capillary-inertial velocity, u_{ci}, expressed as $V_c = 0.76u_{ci}$. Interestingly, substituting the critical center velocity into the formula of Weber number gives a constant value of 0.58. Different with the vertical departure velocity, the horizontal departure velocity appears as a linear relation with the center velocity of the rolling droplet. In addition, with increasing center velocity of the rolling droplet, the jumping directions become more and more parallel to the surface. We expect that these results provide fundamental understanding of droplet jumping dynamics, and could be useful for related engineering applications.

Author information

Corresponding Authors

*E-mail: chu_fuqiang@126.com

*E-mail: d.wen@buaa.edu.cn

Author Contributions

‡F.C. and S.L. contributed equally to this work. The manuscript was written through contributions of all authors. All authors have given approval to the final manuscript.

ORCID

Fuqiang Chu: 0000-0002-4054-143X

Dongsheng Wen: 0000-0003-3492-7982

Notes

The authors declare no competing financial interest.

Acknowledgements

This work was supported by Beijing Natural Science Foundation (No. 3204048), National Postdoctoral Program for Innovative Talents (No. BX20180024), and China Postdoctoral Science Foundation (No. 2019M650444).

References

1. Boreyko, J. B.; Chen, C. H., Self-propelled dropwise condensate on superhydrophobic surfaces. Phys. Rev. Lett. 2009, 103 (18), 184501.
2. Wang, F.-C.; Yang, F.; Zhao, Y.-P., Size effect on the coalescence-induced self-propelled droplet. Appl. Phys. Lett. 2011, 98 (5), 053112.
3. Lv, C.; Hao, P.; Yao, Z.; Niu, F., Departure of condensation droplets on superhydrophobic surfaces. Langmuir 2015, 31 (8), 2414-2420.
4. Enright, R.; Miljkovic, N.; Sprittles, J.; Nolan, K.; Mitchell, R.; Wang, E. N., How Coalescing Droplets Jump. ACS Nano 2014, 8 (10), 10352-10362.
5. Kim, M. K.; Cha, H.; Birbarah, P.; Chavan, S.; Zhong, C.; Xu, Y.; Miljkovic, N., Enhanced Jumping-Droplet Departure. Langmuir 2015, 31 (49), 13452-66.
6. Chu, F.; Wu, X.; Zhu, B.; Zhang, X., Self-propelled droplet behavior during condensation on superhydrophobic surfaces. Appl. Phys. Lett. 2016, 108 (19), 194103.
7. Mouterde, T.; Nguyen, T.-V.; Takahashi, H.; Clanet, C.; Shimoyama, I.; Quéré, D., How merging droplets jump off a superhydrophobic surface: Measurements and model. Phys. Rev. Fluids 2017, 2 (11), 112001(R).
8. Xie, F. F.; Lu, G.; Wang, X. D.; Wang, B. B., Coalescence-Induced Jumping of Two Unequal-Sized Nanodroplets. Langmuir 2018, 34 (8), 2734-2740.
9. Mukherjee, R.; Berrier, A. S.; Murphy, K. R.; Vieitez, J. R.; Boreyko, J. B., How Surface Orientation Affects Jumping-Droplet Condensation. Joule 2019, 3 (5), 1360-1376.
10. Cheng, Y.; Du, B.; Wang, K.; Chen, Y.; Lan, Z.; Wang, Z.; Ma, X., Macrotextures-induced jumping relay of condensate droplets. Appl. Phys. Lett. 2019, 114 (9), 093704.
11. Huang, J.-J.; Huang, H.; Xu, J.-J., Energy-based modeling of micro- and nano-droplet jumping upon coalescence on superhydrophobic surfaces. Appl. Phys. Lett. 2019, 115 (14), 141602.
12. Xie, F. F.; Lu, G.; Wang, X. D.; Wang, D. Q., Enhancement of Coalescence-Induced Nanodroplet Jumping on Superhydrophobic Surfaces. Langmuir 2018, 34 (37), 11195-11203.
13. Wisdom, K. M.; Watson, J. A.; Qu, X.; Liu, F.; Watson, G. S.; Chen, C. H., Self-cleaning of superhydrophobic surfaces by self-propelled jumping condensate. Proc. Natl. Acad. Sci. USA 2013, 110, 7992-7997.
14. Shen, Y.; Jin, M.; Wu, X.; Tao, J.; Luo, X.; Chen, H.; Lu, Y.; Xie, Y., Understanding the frosting and defrosting mechanism on the superhydrophobic surfaces with hierarchical structures for enhancing anti-frosting performance.

Appl. Therm. Eng. 2019, 156, 111-118.
15. Boreyko, J. B.; Zhao, Y. J.; Chen, C. H., Planar jumping-drop thermal diodes. Appl. Phys. Lett. 2011, 99 (23), 234105.
16. Hao, Q.; Pang, Y.; Zhao, Y.; Zhang, J.; Feng, J.; Yao, S., Mechanism of delayed frost growth on superhydrophobic surfaces with jumping condensates: more than interdrop freezing. Langmuir 2014, 30 (51), 15416-22.
17. Chu, F.; Wu, X.; Wang, L., Dynamic melting of freezing droplets on ultraslippery superhydrophobic surfaces. ACS Appl. Mater. Interfaces 2017, 9, 8420-8425.
18. Chu, F.; Wen, D.; Wu, X., Frost Self-Removal Mechanism during Defrosting on Vertical Superhydrophobic Surfaces: Peeling Off or Jumping Off. Langmuir 2018, 34 (48), 14562-14569.
19. Miljkovic, N.; Enright, R.; Nam, Y.; Lopez, K.; Dou, N.; Sack, J.; Wang, E. N., Jumping-droplet-enhanced condensation on scalable superhydrophobic nanostructured surfaces. Nano Lett. 2013, 13 (1), 179-187.
20. Wen, R.; Xu, S.; Ma, X.; Lee, Y.-C.; Yang, R., Three-Dimensional Superhydrophobic Nanowire Networks for Enhancing Condensation Heat Transfer. Joule 2018, 2 (2), 269-279.
21. Lu, M.-C.; Lin, C.-C.; Lo, C.-W.; Huang, C.-W.; Wang, C.-C., Superhydrophobic Si nanowires for enhanced condensation heat transfer. Int. J. Heat Mass Transfer 2017, 111, 614-623.
22. Boreyko, J. B.; Collier, C. P., Delayed frost growth on jumping-drop superhydrophobic surfaces. ACS Nano 2013, 7 (2), 1618-1627.
23. Wiedenheft, K. F.; Guo, H. A.; Qu, X.; Boreyko, J. B.; Liu, F.; Zhang, K.; Eid, F.; Choudhury, A.; Li, Z.; Chen, C.-H., Hotspot cooling with jumping-drop vapor chambers. Appl. Phys. Lett. 2017, 110 (14), 141601.
24. Liu, F.; Ghigliotti, G.; Feng, J. J.; Chen, C.-H., Numerical simulations of self-propelled jumping upon drop coalescence on non-wetting surfaces. J. Fluid Mech. 2014, 752, 39-65.
25. Liu, F.; Ghigliotti, G.; Feng, J. J.; Chen, C.-H., Self-propelled jumping upon drop coalescence on Leidenfrost surfaces. J. Fluid Mech. 2014, 752, 22-38.
26. Wang, K.; Li, R. X.; Liang, Q. Q.; Jiang, R.; Zheng, Y.; Lan, Z.; Ma, X. H., Critical size ratio for coalescence-induced droplet jumping on superhydrophobic surfaces. Appl. Phys. Lett. 2017, 111 (6), 061603.
27. Lecointre, P.; Mouterde, T.; Checco, A.; Black, C. T.; Rahman, A.; Clanet, C.; Quere, D., Ballistics of self-jumping microdroplets. Phys. Rev. Fluids 2019, 4 (1), 013601.
28. Liu, X.; Cheng, P., 3D multiphase lattice Boltzmann simulations for morphological effects on self-propelled jumping of droplets on textured superhydrophobic surfaces. Int. Commun. Heat Mass Transfer 2015, 64, 7-13.
29. Attarzadeh, R.; Dolatabadi, A., Coalescence-induced jumping of micro-droplets on heterogeneous superhydrophobic surfaces. Phys. Fluids 2017, 29 (1), 012104.
30. Mulroe, M. D.; Srijanto, B. R.; Ahmadi, S. F.; Collier, C. P.; Boreyko, J. B., Tuning Superhydrophobic Nanostructures To Enhance Jumping-Droplet Condensation. ACS Nano 2017, 11 (8), 8499-8510.
31. Zhang, P.; Maeda, Y.; Lv, F. Y.; Takata, Y.; Orejon, D., Enhanced Coalescence-Induced Droplet-Jumping on Nanostructured Superhydrophobic Surfaces in the Absence of Microstructures. ACS Appl. Mater. Interfaces 2017, 9 (40), 35391-35403.
32. Lv, C. J.; Hao, P. F.; Yao, Z. H.; Song, Y.; Zhang, X. W.; He, F., Condensation and jumping relay of droplets on lotus leaf. Appl. Phys. Lett. 2013, 103 (2), 021601.
33. Yuan, Z.; Wu, R.; Wu, X., Numerical simulations of multi-hop jumping on superhydrophobic surfaces. Int. J. Heat Mass Transfer 2019, 135, 345-353.
34. Chen, Y.; Lian, Y. S., Numerical investigation of coalescence-induced self-propelled behavior of droplets on non-wetting surfaces. Phys. Fluids 2018, 30 (11), 112102.
35. Liu, J.; Guo, H.; Zhang, B.; Qiao, S.; Shao, M.; Zhang, X.; Feng, X. Q.; Li, Q.; Song, Y.; Jiang, L.; Wang, J., Guided Self-Propelled Leaping of Droplets on a Micro-Anisotropic Superhydrophobic Surface. Angewandte Chemie 2016, 55 (13), 4265-4269.
36. Yuan, Z.; Hu, Z.; Chu, F.; Wu, X., Enhanced and guided self-propelled jumping on the superhydrophobic surfaces with macrotexture. Appl. Phys. Lett. 2019, 115 (16), 163701.

37. Li, S.; Chu, F.; Zhang, J.; Brutin, D.; Wen, D., Droplet jumping induced by coalescence of a moving droplet and a static one: Effect of initial velocity. Chem. Eng. Sci. 2020, 211, 115252.
38. Xie, J.; Xu, J.; Shang, W.; Zhang, K., Mode selection between sliding and rolling for droplet on inclined surface: Effect of surface wettability. Int. J. Heat Mass Transfer 2018, 122, 45-58.
39. Xie, J.; Xu, J.; Shang, W.; Zhang, K., Dropwise condensation on superhydrophobic nanostructure surface, part II: Mathematical model. Int. J. Heat Mass Transfer 2018, 127, 1170-1187.
40. Chu, F.; Wu, X., Fabrication and condensation characteristics of metallic superhydrophobic surface with hierarchical micro-nano structures. Appl. Surf. Sci. 2016, 371, 322-328.
41. Chu, F.; Gao, S.; Zhang, X.; Wu, X.; Wen, D., Droplet re-icing characteristics on a superhydrophobic surface. Appl. Phys. Lett. 2019, 115 (7), 073703.
42. Chu, F.; Zhang, X.; Li, S.; Jin, H.; Zhang, J.; Wu, X.; Wen, D., Bubble formation in freezing droplets. Phys. Rev. Fluids 2019, 4 (7), 071601(R).
43. Xie, J.; Xu, J.; Liu, Q.; Li, X., Coupling Diffusion Welding Technique and Mesh Screen Creates Heterogeneous Metal Surface for Droplets Array. Adv. Mater. Interfaces 2017, 4 (23), 1700684.
44. Thoroddsen, S. T.; Etoh, T. G.; Takehara, K.; Ootsuka, N.; Hatsuki, Y., The air bubble entrapped under a drop impacting on a solid surface. J. Fluid Mech. 2005, 545, 203-212.
45. Yan, X.; Zhang, L.; Sett, S.; Feng, L.; Zhao, C.; Huang, Z.; Vahabi, H.; Kota, A. K.; Chen, F.; Miljkovic, N., Droplet Jumping: Effects of Droplet Size, Surface Structure, Pinning, and Liquid Properties. ACS Nano 2019, 13 (2), 1309-1323.

Table of contents